

EXPERIMENTAL INVESTIGATION OF SUBCOOLED FLOW BOILING OF WATER/TiO₂ NANOFLUID IN A HORIZONTAL TUBE

by

Hossein RAJABNIA*, **Ehsan ABEDINI**, **Ali TAHMASBI**,
and Amin BEHZADMEHR

Mechanical Engineering Department, University of Sistan and Baluchestan, Zahedan, Iran

Original scientific paper
DOI: 10.2298/TSCI130929122R

Subcooled flow boiling heat transfer of water/TiO₂ nanofluid in a horizontal tube is experimentally investigated. To validate the experimental apparatus as well as the experimental procedure, data for distilled water were compared with the available results on the literature in both single phase and subcooled flow boiling regime. Experimental investigations were carried out at three nanoparticles volumetric concentrations of 0.01%, 0.1%, and 5%. It was found that the nanofluid heat transfer coefficient in single-phase flow regime augments with the nanoparticle concentration. However, in the case of subcooled flow boiling regime the heat transfer coefficient decreases with the nanoparticle volume fractions.

Key words: *nanofluid, subcooled flow boiling, heat transfer coefficient*

Introduction

High performance thermal devices, to be small in size and light in weight, are of great importance for different industries. Low thermal conductivity of conventional fluids is one of the main obstacles to have such devices. Maxwell's study [1] shows the possibility of increasing the thermal conductivity of a fluid-solid mixture by increasing volume fraction of solid particles. Choi *et al.* [2] is the first who used the term of nanofluids to refer to a fluid with suspended nanoparticles. According to their results the thermal conductivity of fluid with suspended particles are expected to be higher than those of common fluids. Several researchers such as Masuda *et al.* [3], Lee *et al.* [4], Xuan and Li [5], and Xuan and Roetzel [6] investigated the effect of nanoparticle concentrations on the thermal characteristics of the nanofluids. These works show that the thermal conductivity of nanofluid increases with the nanoparticle concentrations. It is also shown that the heat transfer coefficient augments with the nanoparticle volume fractions. Wen and Ding [7] measured the thermal conductivity of nanofluid with different nanoparticles volume fractions, material, and mean particle size in several base fluids. All findings showed that the thermal conductivity of nanofluid is higher than the base fluids. They also reported an enhancement on the heat transfer coefficient which is not only due to thermal conductivity augmentation but also the particles' movement. Mirmasumi and Behzadmehr [8] numerically studied the influence of nanoparticles mean diameter on the convection heat transfer coefficient in a horizontal tube. They showed that the convection heat transfer coefficient significantly increases with decreasing mean diameter of the nanoparticles.

* Corresponding author; e-mail: ho.rajabnia@gmail.com

On the other hand, boiling is known as the most efficient mode of heat transfer. There are many variables that influence boiling heat transfer. As it is identified by Rohsenow and Griffith [9] these variables are surface parameters, fluid properties, and surface-fluid interactions. However, using nanofluid in a boiling mechanism adds a third (solid) phase into an already existing two phase (liquid-vapour) system. Investigation in convective flow boiling of nanofluids has become interesting in recent years for which high-heat flux cooling or compact heat exchangers is necessary for applications such as microelectronics devices. Some studies reported heat transfer coefficient enhancement in pool boiling. However other investigations showed degradation of nucleate boiling heat transfer coefficient in nanofluids.

Das *et al.* [10] investigated on the pool boiling of nanofluids. Their results indicated that the particles have important effects on the boiling process. Their experimental work shows that the nucleate boiling deteriorated and thus the surface temperature augmented with increasing nanoparticle concentrations because of changing the surface characteristics. Liu *et al.* [11] showed that the heat transfer increases by using carbon nanotubes/water in pool boiling process.

Table 1. Summary of some investigations on boiling of nanofluid

Nanofluid	Authors	Boiling geometry	Results
Al ₂ O ₃ /water [13]	Prakash <i>et al.</i>	Vertical tubular heater	BHT increases with rough heater surface and decreases with smooth surface
Al ₂ O ₃ /water [14], 0.32, 0.71, 0.95, 1.25 wt.%	Wen and Ding	Horizontal SS plate, D = 150 mm	BHT enhanced by 10-40%
TiO ₂ /water [15] 0.00005-0.01 vol.%	Suriyawong and Wongwises	Horizontal circular plates – Cu & Al. Sizes unspecified Ra = 0.2-4 μm	BHT is always increased, depending on φ and roughness. On Al plate, BHT always deteriorated
CNT/water, CNT-R22 [16] 0-1 vol.%	Park and Jung	Horizontal plain tube D = 19 mm, L = 152 mm	BHT enhanced depending on heat flux and φ
Al ₂ O ₃ /water [17]	Abedini <i>et al.</i>	D = 10 mm	BHT enhanced depending on heat flux and φ
SiO ₂ /water [18] 0.5-0.67 vol.%	Vassallo <i>et al.</i>	Horizontal NiCr wire D = 0.4 mm, L = 75 mm	No enhancement in BHT, but CHF increase up to 60%
Al ₂ O ₃ /water, Al ₂ O ₃ /ethanol [19] 0.0001 wt.%-1 wt.%	Coursey and Kim	Horizontal circular Cu surface 0.9 cm ²	BHT no change or degrade
Al ₂ O ₃ /water, Al ₂ O ₃ / ZnO, Al ₂ O ₃ -water-EG [20] 0-0.5g/l	Moreno <i>et al.</i>	Horizontal Cu block 10 × 10 × 3 mm	CHF enhanced in all cases. BHT unchanged or deteriorated depending on heat flux
Al ₂ O ₃ /water [21] 0.5, 1, 2, 4 vol.%	Bang and Chang	Horizontal & vertical Cu flat surface, 4 × 100 mm ²	BHT deteriorated, CHF enhanced and more on horizontal
Cu/water & Cu/SDS-water [22] Cu 0.25%, 0.5%, and 1.0 wt.%, SDS 9 wt.%	Kathiravan <i>et al.</i>	Stainless steel test-heater surface of 30 mm size and 0.44 mm thickness	CHF increased. BHT deteriorated
Carbon nanotubes (CNT) [23]	Sujith <i>et al.</i>	Mini-channel	CHF increased

Kwark *et al.* [12] investigated pool boiling of Al_2O_3 , CuO, and diamond nanoparticles in water. They observed that the boiling heat transfer coefficient does not change. Table 1 shows a brief biography on the boiling heat transfer studies. In this table, some works show enhancement of heat transfer, [13-17] some others show deterioration of heat transfer, [21-23] and few works show little change or no change of heat transfer [18, 20]. It should be mention that the critical heat flux (CHF) increases in all experimental investigations on nanofluids, even in the cases where the boiling heat transfer reduces.

The work of Kim *et al.* [24, 25] is one of the few works in subcooled flow boiling of nanofluids. They used dilute alumina, zinc oxide, and diamond nanofluids at atmospheric pressure to investigate the flow boiling heat transfer coefficient. Although their results showed enhancement in critical heat flux of nanofluids, the heat transfer coefficient did not change and even decreased. By confocal microscopy-based examination of the test section, they claimed that deposition on the boiling surface has led to change of nucleation sites and the wettability of surface. It is widely agreed among the majority of researchers that the boiling heat transfer and CHF behavior of nanofluids are basically influenced by the changes on heated surface as result of nanoparticle deposition. Hormozi and Sarafraz [26] investigated the convection heat transfer of CuO/water nanofluid in both forced convective and subcooled flow boiling conditions. Their results showed that heat transfer decreases in both conditions.

The aim of this article is to investigate the effect of nanofluids on the subcooled flow boiling heat transfer coefficient along a horizontal tube.

Flow boiling experimental set-up

Figure 1 schematically shows the experimental set-up to measure the convective heat transfer coefficient. The experimental apparatus is composed of a cooling system, a test section, a power supply, a measurement system, and a data acquisition system. The test section is resistively heated using DC power supply with 10 V and 500 A output voltage and current respectively which is connected to the tube ends by copper electrodes. The test section of the experimental apparatus is an horizontal circular tube which is made of a stainless steel grade 316 with inner diameter of 10 mm, wall thickness of 1.0 mm and effective length of 1000 mm.

Wall temperatures along the tube length are measured using 15 type K thermocouples mounted on the tube external surface. They are electrically insulated from the tube surface by using low conductivity material (mica sheet with 0.1 mm thickness) to prevent any interference between the thermocouples and the DC current passing through the tube.

The thermocouples are mounted at five axial positions along the tube length. The temperatures are recorded by a data acquisition system. Fluid bulk temperature at the inlet and outlet of the test section are measured by using pt-100 sensors which are mounted in two calming chambers. To achieve a steady-state condition, the inlet temperature of the liquid is controlled and fixed by using an automated preheater. The tube was covered with a fibre-glass pipe insulating material to reduce the heat loss. In the case of single-phase water flow the heat loss is generally less than $\pm 2\%$ of the total power input. After 40 minutes of system warm

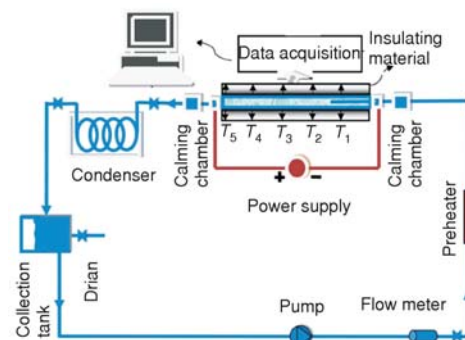


Figure 1. Schematic representation of the flow system

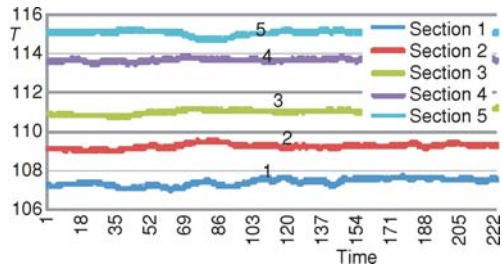


Figure 2. Average wall temperature at the steady-state conditions

up steady-state condition is achieved. Data is recorded over a period of more than 200 second for each test.

Figure 2 shows that over this period of time the variation of temperatures is negligible. It should be mentioned that each line presents the average value of three thermocouples which were mounted on a particular section.

The heat flux was calculated using this following equation:

$$Q^* = \frac{VI}{\pi DL} \quad (1)$$

where V and I are the measured voltage and current, and D and L are the test section inner diameter and the length, respectively.

The heat transfer coefficient is calculated by applying Newton's law of cooling:

$$h_{\text{eff}}(x) = \frac{Q^*}{T_w(x) - T_b(x)} \quad (2)$$

where T_w is the average of surface temperature recorded by thermocouples mounted on the surface, and T_b is the local mean liquid temperature which can be calculated from the energy balance equation:

$$T_b(x) = T_{\text{bi}} + \frac{PQ''}{\dot{m}c} x \quad (3)$$

where c is the specific heat, \dot{m} – the mass flux, P – the perimeter of the tube, and T_{bi} – the inlet liquid temperature which it is measured using PT-100 thermocouples.

Nanofluid preparation and characterization

The nanoparticles used in these experiments are TiO_2 particles with mean diameter of 20 nm and purity of 99%. The base working fluid is pure water because boiling characteristics of the base fluid (water) is well known and the TiO_2 nanoparticles are commercially available. No surfactant or buffer was added in the nanofluids during dispersion process. Mixture of nanoparticles and the base fluid was sonicated with an ultrasonic prob for an hour to obtain nanofluid.



Figure 3. The nanofluids used during the tests

Nanofluids were prepared in three volume fractions (0.01%, 0.1%, and 0.5%) with considered apparent density. The nanofluid was found stable over a week for 0.1 vol.%. The prepared nanofluid in 0.01 and 0.1% concentrations is shown in fig. 3.

Uncertainty analysis

The uncertainties of the measured parameters are analyzed by the error propagation method [27]. As shown in tab. 2, value for uncertainty of

the temperature and the heat transfer coefficient are estimated by 0.8 °C and 0.065, 0.065, respectively. The following equations are used for uncertainty calculation:

$$dT_b = dT_{in} + (T_b - T_{in}) \left(\frac{dq}{q} + \frac{d\dot{m}}{\dot{m}} \right) \quad (4)$$

$$\frac{dh}{h} = \frac{dq}{q} + \frac{dT_w}{T_w - T_b} + \frac{dT_b}{T_w - T_b} \quad (5)$$

Table 2. Uncertainty of the measured parameter

Parameter	Uncertainty [%]
dT_{in}	0.1
dq	1.5
$d\dot{m}$	0.02
dT_w	0.7

Experiment

The experiments conducted in atmospheric pressure throughout a horizontal tube. The heat transfer coefficient was measured in subcooled flow boiling and single phase regimes for both pure water and nanofluids with different concentrations (0.01%, 0.1%, and 0.5%) and different mass fluxes ($G = 138, 210, \text{ and } 308 \text{ kg/m}^2\text{s}$).

Validation of experimental set-up

In addition to the calibration of each sensor, several tests were performed to validate the set-up for both single phase and two phase regimes. In the case of single phase flow regime, the measured values were compared with the well-known Gnielinski correlation [28]. As shown in figs. 4 and 5, the difference between the experimental data and the Gnielinski correlation is about 8%.

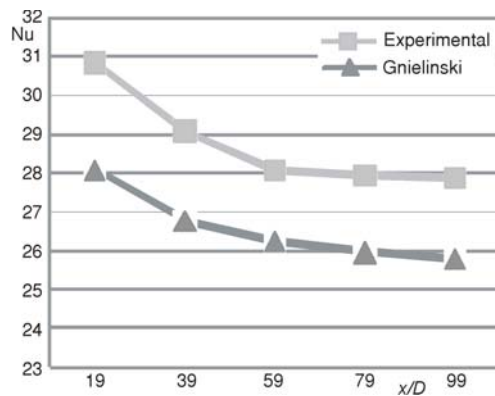


Figure 4. Comparison of the experimental result with Gnielinski correlation [28] in horizontal tube, $Q'' = 38.85 \text{ kW/m}^2$, $G = 210 \text{ kg/m}^2\text{s}$

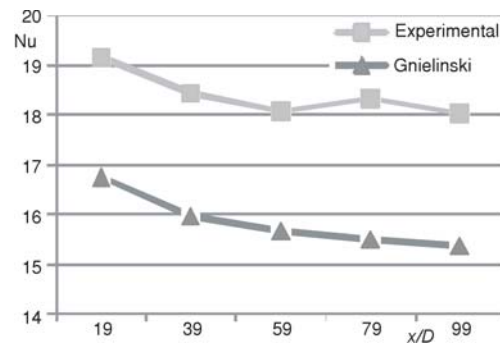


Figure 5. Comparison of the experimental result with Gnielinski correlation [28] in horizontal tube, $Q'' = 26.75 \text{ kW/m}^2$, $G = 138 \text{ kg/m}^2\text{s}$

In the case of subcooled flow boiling regime the measured values were compared with the predicted results of Chen [29] which is defined by the following equation:

$$Q'' = h_{FC}(T_w - T_b) + h_{NB}(T_w - T_{sat}) \quad (6)$$

where h_{FC} and h_{NB} are the heat transfer coefficients due to forced convection and nucleate boiling, respectively:

$$h_{NB} = 0.00122 \left[\frac{k_f^{0.79} C_{p,f}^{0.45} \rho_f^{0.49}}{\sigma^{0.5} \mu_f^{0.29} h_{fg}^{0.24} \rho_g^{0.24}} \right] (T_w - T_{sat})^{0.24} (P - P_{sat})^{0.75} S \quad (7)$$

$$h_{FC} = \left(\frac{K_l}{D} \right) 0.023 \left[\frac{G(1-X)D}{\mu} \right]^{0.8} \left(\frac{\mu C_p}{K_l} \right)^{0.4} F \quad (8)$$

The nucleate boiling suppression parameter, S , is:

$$S = \frac{1}{1 + 2.53 \cdot 10^6 \left\{ \left[G(1-X) \frac{D}{\mu_l} \right] F^{1.25} \right\}^{1.17}} \quad (9)$$

Wall temperature is calculated using an iterative procedure. The results compare with the experimental results. As shown in figs. 6 and 7, good concordance between the results is observed.

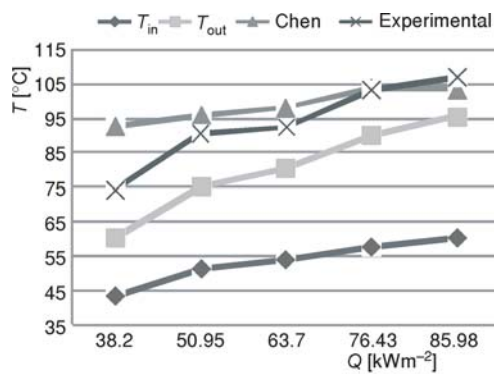


Figure 6. Temperature vs. heat flux curves for pure water at $G = 210 \text{ kg/m}^2\text{s}$

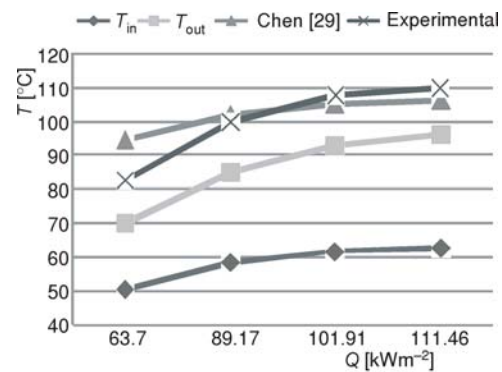


Figure 7. Temperature vs. heat flux curves for pure water at $G = 302 \text{ kg/m}^2\text{s}$

Results and discussion

In the case of single phase nanofluid flow regime, as seen in figs. 8 and 9 a positive effect on the heat transfer coefficient is observed. It is clearly shown that the local convective heat transfer coefficient augments with increasing nanoparticles concentration. It is in good agreement with the results have been obtained by other researchers. Several reasons have been proposed for such enhancement. Among these reasons could be mentioned to the mixing effects of particles near the wall, Brownian motion of particles, thermal conductivity increment, particle migration, reduction of boundary layer thickness, and delay in boundary layer development [8, 30, 31]. However, contrary to the

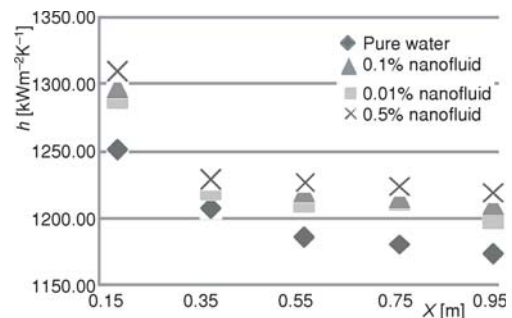


Figure 8. Effective heat transfer coefficient of water and TiO_2 nanofluids with single phase flow at $Q'' = 25.5 \text{ kW/m}^2$, $G = 138 \text{ kg/m}^2\text{s}$

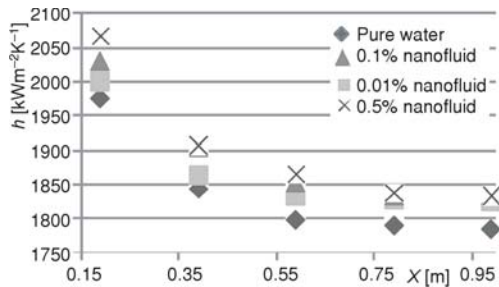


Figure 9. Effective heat transfer coefficient of water and TiO₂ nanofluids with single phase flow at $Q'' = 38.8 \text{ kW/m}^2$, $G = 210 \text{ kg/m}^2\text{s}$

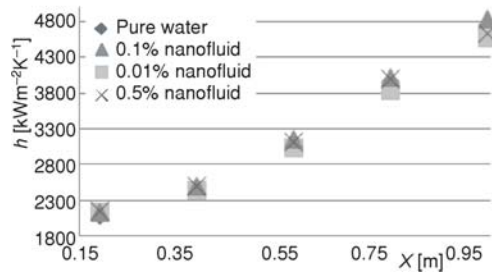


Figure 10. Effective heat transfer coefficient of water and TiO₂ nanofluids with subcooled flow boiling at $Q'' = 63.7 \text{ kW/m}^2$, $G = 138 \text{ kg/m}^2\text{s}$

single phase flow regime, the results in subcooled flow boiling indicate deterioration in the convective heat transfer coefficient compared to the one for distilled water.

Figures 10-12 show subcooled flow boiling heat transfer coefficients at three different mass fluxes: $G = 138, 210,$ and $302 \text{ kg/m}^2\text{s}$, respectively. As seen in these figures, in the case of subcooled flow boiling regime, in general the heat transfer coefficient does not improve with using nanofluid. Figures 13-15 clearly show such comparisons along the tube length. The results show that the variations of effective heat transfer coefficient in these cases are within the range

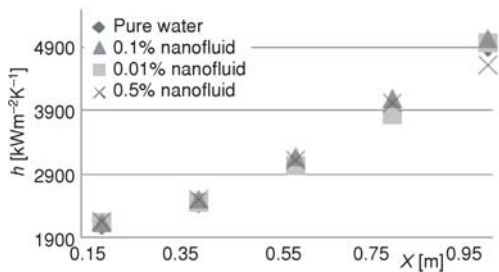


Figure 11. Effective heat transfer coefficient of water and TiO₂ nanofluids with subcooled flow boiling at $Q'' = 84.7 \text{ kW/m}^2$, $G = 210 \text{ kg/m}^2\text{s}$

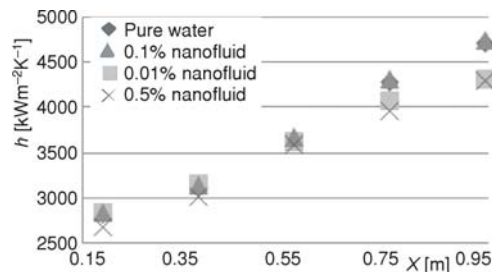


Figure 12. Effective heat transfer coefficient of water and TiO₂ nanofluids with subcooled flow boiling at $Q'' = 101.91 \text{ kW/m}^2$, $G = 308 \text{ kg/m}^2\text{s}$

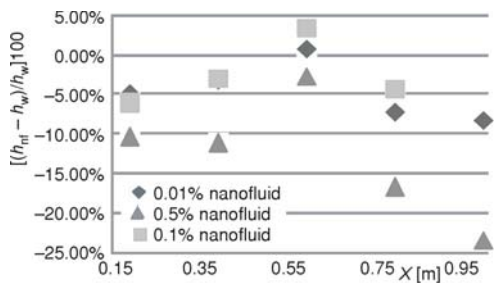


Figure 13. Ratio of effective heat transfer coefficient of water and TiO₂ nanofluids with subcooled flow boiling at $Q'' = 63.7 \text{ kW/m}^2$, $G = 138 \text{ kg/m}^2\text{s}$

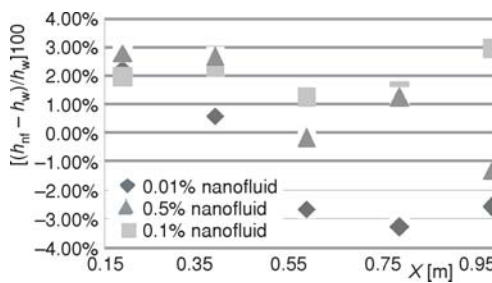


Figure 14. Ratio of effective heat transfer coefficient of water and TiO₂ nanofluids with subcooled flow boiling at $Q'' = 84.7 \text{ kW/m}^2$, $G = 210 \text{ kg/m}^2\text{s}$

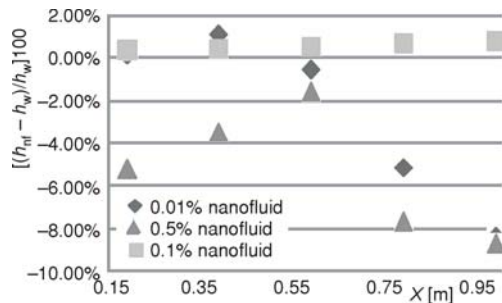


Figure 15. Ratio of effective heat transfer coefficient of water and TiO₂ nanofluids with subcooled flow boiling at $Q'' = 101.91 \text{ kW/m}^2$, $G = 308 \text{ kg/m}^2\text{s}$

of accuracy of the measured data. As shown in tab. 3, the average heat transfer coefficient through the tube does not significantly vary with using nanoparticles.

It may arise from the fact that using nanoparticles affect the formation, number and size of the generated bubbles at the surface. In addition, some irregularities that are seen on the results could be because of the nanoparticle sedimentation at the tube inner surface. The nanoparticle sedimentation generates a very rough surface with random roughness. The latter results random surface contact angles in contact with a liquid flow and changes the surface

wettability[32, 33] as well as the number of microcavities.

Results show that the more concentration increases, the more boiling heat transfer of nanofluid decreases. Nanoparticle deposition changes the surface roughness and number of microcavities presence on the surface. Although direct measurement of the nucleation site density which plays the most important role in boiling heat transfer is impossible, it seems that with increasing nanoparticles concentration, more deposition of nanoparticles occurs. The latter changes the surface roughness and also the microcavities. If deposition of large particles, on surfaces with relatively small cavities, occurs it could create more nucleate sites and then generate more vapor bubbles.

Table 3. Ratio of effective heat transfer coefficient of water and TiO₂ nanofluids with subcooled flow boiling

	$G = 138 \text{ kg/m}^2\text{s}$	$G = 210 \text{ kg/m}^2\text{s}$			$G = 308 \text{ kg/m}^2\text{s}$	
	$Q'' = 63.746 \text{ [kWm}^{-2}\text{]}$	$Q'' = 63.6946 \text{ [kWm}^{-2}\text{]}$	$Q'' = 76.43346 \text{ [kWm}^{-2}\text{]}$	$Q'' = 84.746 \text{ [kWm}^{-2}\text{]}$	$Q'' = 101.91 \text{ [kWm}^{-2}\text{]}$	$Q'' = 111.46 \text{ [kWm}^{-2}\text{]}$
0.01%	-0.0459	0.0074	0.0047	-0.01132	-0.0255	-0.0213
0.1%	-0.0633	-0.0095	-0.0342	0.020039	0.0056	-0.0524
0.5%	-0.12875	-0.0094	-0.0371	0.01061	-0.0622	-0.0689

Conclusions

Experimental investigation of subcooled flow boiling heat transfer has been conducted on stainless steel tubes with different concentrations of water/TiO₂ nanofluids. Contrary to single phase flow regime, the experimental data shows that by increasing the nanoparticles concentration the average heat transfer coefficient in subcooled flow boiling regimes slightly decreases. Since the bubble formations are affected due to changing the surface characteristic as result of nanoparticles deposition. Furthermore, based on the experimental results, it is not recommended to use nanofluids for enhancing the heat transfer coefficient in subcooled flow boiling. However, more investigation is needed to elucidate the link between the boiling curve shift and nanoparticle deposition.

Nomenclature

c – specific heat, [$\text{Jkg}^{-1}\text{K}^{-1}$]

D – diameter, [m]

G	– mass flux, [$\text{kgm}^{-2}\text{s}^{-1}$]
h	– specific enthalpy, [Jkg^{-1}]
I	– current, [A]
k	– thermal conductivity, [WMk^{-1}]
L	– tube heater length, [m]
l	– liquid phase
p	– pressure, [Pa]
q	– heat flux, [Wm^{-2}]
Ra	– average roughness, [μm]
S	– nucleate boiling suppression parameter
T	– temperature, [K]
V	– voltage, [V]
x	– distance, [m]

Greek symbols

μ	– viscosity [Nsm^{-2}]
ρ	– density [kgm^{-3}]
σ	– surface tension [Nm^{-1}]
φ	– nanoparticles volume fraction

Acronyms

BHT	– boiling heat transfer
CHF	– critical heat flux

Subscripts

b	– bulk liquid
f	– liquid phase at saturation condition
fg	– liquid-to-vapour transition at saturated condition
g	– vapour phase at saturated condition
eff	– effective
in	– inner
l	– liquid phase
O	– outer
P	– constant pressure
sat	– saturation
w	– wall

References

- [1] Maxwell, J. C., *Electricity and Magnetism*, Clarendon Press, Oxford, UK, 1873
- [2] Choi, S. U. S., et al., Anomalous Thermal Conductivity Enhancement in Nano-Tube Suspensions, *Applied Physics Letters*, 79 (2001), 14, pp. 2252-2254
- [3] Masuda, H., et al., Conductivity and Viscosity of Liquid by Dispersed Ultra-Fine Particles (Dispersion of Al_2O_3 , SiO_2 , and TiO_2 Ultra-Fine Particles), *Alteration of Thermal, Netsu Bussei (Japan)* 7 (1993), 4, pp. 227-233
- [4] Lee, S., et al., Measuring Thermal Conductivity of Fluids Containing Oxide Nanoparticles, *Journal of Heat Transfer*, 121 (1999), May, pp. 280-2899
- [5] Xuan, Y., Li, Q., Investigation on Convective Heat Transfer and Flow Features of Nanofluids, *ASME J. Heat Transfer*, 125 (2003), 1, pp. 125-151
- [6] Xuan, Y., Roetzel, W., Conceptions for Heat Transfer Correlation of Nanofluids, *International Journal of Heat and Mass Transfer*, 43 (2000), 19, pp. 3701-3707
- [7] Wen, D., Ding, Y., Experimental Investigation into the Pool Boiling Heat Transfer of Aqueous Based -Alumina Nanofluids, *J Nanopart*, 7 (2005), 2, pp. 265-274
- [8] Mirmasoumi, S., Behzadmehr, A., Effect of Nanoparticles Mean Diameter on Mixed Convection Heat Transfer of a Nanofluid in a Horizontal Tube, *International Journal of Heat and Fluid Flow*, 29 (2007), 2, pp. 557-566
- [9] Rohsenow, W. M., Griffith, P., Correlation of Maximum Heat Flux Data for Boiling of Saturated Liquids, *Chemical Engineering Progress Symposium*, 52 (1956), pp. 47-49
- [10] Das, S. K., et al., Pool Boiling Characteristics of Nano-Fluids, *International Journal of Heat and Mass Transfer*, 46 (2003), 5, pp. 851-862
- [11] Liu, Z. H., et al., Boiling Characteristics of Carbon Nanotube Suspensions under Sub-Atmospheric Pressures, *Int J Therm Sci.*, 49 (2010), 7, pp. 1156-1164
- [12] Kwark, S. M., et al., Pool Boiling Characteristics of Low Concentration Nanofluids, *Int J Heat Mass Transfer*, 53 (2010), 5-6, pp. 972-981
- [13] Prakash, N. G., et al., Mechanism of Enhancement/Deterioration of Boiling Heat Transfer Using Stable Nanoparticles Suspensions over Vertical Tubes, *J Appl Phys*, 102 (2007), 7, pp. 074317-1-074317-7
- [14] Wen, D. S., et al., Pool Boiling Heat Transfer of Aqueous TiO_2 - Based Nanofluids, *Journal of Enhanced Heat Transfer*, 13 (2006), 3, pp. 231-244
- [15] Suriyawong, A., Wongwiset, S., Nucleate Pool Boiling Heat Transfer Characteristics of TiO_2 -Water Nanofluids at Very Low Concentrations, *Experimental Thermal and Fluid Science*, 34 (2010), 8, pp. 992-999
- [16] Park, K. J., Jung, D. S., Enhancement of Nucleate Boiling Heat Transfer Using Carbon Nanotubes, *International Journal of Heat and Mass Transfer*, 50 (2007), 21-22, pp. 4499-4502

- [17] Abedini, E., et al., Numerical Investigation of Subcooled Flow Boiling of a Nanofluid, *International Journal of Thermal Sciences*, 64 (2013), Feb., pp. 232-239
- [18] Vassallo, P., et al., Pool Boiling Heat Transfer Experiments in Silica-Water Nano-Fluids, *International Journal of Heat and Mass Transfer*, 47 (2004), 2, pp. 407-411
- [19] Coursey, J. S., Kim, J., Nanofluid Boiling: The Effect of Surface Wettability, *International Journal of Heat and Fluid Flow*, 29 (2008), 6, pp. 1577-1585
- [20] Moreno, G., et al., Pool Boiling Heat Transfer of Alumina-Water, Zinc Oxide-Water and Alumina-Water Plus Ethylene Glycol Nanofluids, in: Ht2005, *Proceedings*, ASME Summer Heat Transfer Conference, San Francisco, Cal., USA, 2005, Vol. 2, pp. 625-632
- [21] Bang, I. C., Chang, S. H., Boiling Heat Transfer Performance and Phenomena of Al₂O₃-Water Nano-Fluids from a Plain Surface in a Pool, *International Journal of Heat and Mass Transfer*, 48 (2005), 12, pp. 2407-2419
- [22] Kathiravan, R., et al., Preparation and Pool Boiling Characteristics of Copper Nanofluids over a Flat Plate Heater, *Journal of Heat and Mass Transfer*, 53 (2010), 9-10, pp. 1673-1681
- [23] Sujith Kumar, C. S., et al., Flow Boiling Heat Transfer Enhancement Using Carbon Nanotube Coatings, *Applied Thermal Engineering*, 65 (2014), 1-2, pp. 166-175
- [24] Kim, S. J., et al., Subcooled Flow Boiling Heat Transfer of Dilute Alumina, Zinc Oxide, and Diamond Nanofluids at Atmospheric Pressure, *Nucl Eng Des*, 240 (2010), 5, pp. 1186-1194
- [25] Kim, S. J., et al., Experimental Study of Flow Critical Heat Flux in Alumina-Water, Zinc-Oxide-Water and Diamond-Water Nanofluids, *J. Heat Transfer*, 131 (2009), 4, pp. 043204-043210
- [26] Hormozi, F., Sarafraz, M. M., Scale Formation and Subcooled Flow Boiling Heat Transfer of CuO-Water Nanofluid Inside the Vertical Annulus, *Experimental Thermal and Fluid Science*, 52 (2014), Jan., pp. 205-214
- [27] ***, ANSI/ASME PTC 19.1, ASME Performance Test Codes: Supplement on Instruments and Apparatus, Part I: Measurement Uncertainty, 1985
- [28] Gnielinski, V., New Equations for Heat and Mass Transfer in Turbulent Pipe and Channel Flow, *Int Chem Eng*, 16 (1976), Jan., pp. 359-368
- [29] Chen, J. C., Correlation for Boiling Heat Transfer to Saturated Fluids in Convective Flow, *Ind Eng Chem Process Des Dev*, 5 (1966), 3, pp. 322-329
- [30] Batchelor, G. K., The Effect of Brownian Motion on the Bulk Stress in a Suspension of Spherical Particles, *J. Fluid Mech.*, 83 (1977), 1, pp. 97-117
- [31] Maiga, S. E. B., et al., Heat Transfer Enhancement by Using Nanofluids in Forced Convection Flows, *International Journal of Heat and Fluid Flow*, 26 (2005), 4, pp. 530-546
- [32] Kim, S. J., et al., Surface Wettability Change during Pool Boiling of Nanofluids and its Effect on Critical Heat Flux, *Int. J. Heat Mass Transfer*, 50 (2007), 19-20, pp. 4105-4116
- [33] Kim, S. J., et al., Effects of Nanoparticle Deposition on Surface Wettability Influencing Boiling Heat Transfer in Nanofluids, *Appl. Phys. Lett.*, 89 (2007), 15, pp. 153107-153109